

Top-Quark Properties at the LHC

K. Beernaert on behalf of the ATLAS and CMS collaborations
*DESY CMS, Notkestraße 85,
 22607 Hamburg, Germany*

A review of recent measurements of top-quark properties is presented. Inclusive and differential top-quark pair charge asymmetry measurements using the full Run I dataset are found to be in agreement with the standard model (SM) predictions. Results of spin correlation in top-quark pairs are presented and interpreted in terms of the SM predicted values and new physics models. Limits are set on flavour-changing neutral currents (FCNC), in particular with a Higgs boson in the final state.

1 Introduction

Due to its short lifetime, the top quark decays before it can form bound states and before its spin decorrelates. As a consequence we can study "bare" quark properties. The top quark has a mass of approximately 173 GeV and may play a significant role in electro-weak symmetry breaking due to its large coupling to the Higgs boson. Measurements of the top-quark properties with increasing levels of precision test the SM and open the possibility to probe new physics. The data used for the studies presented here were collected in pp collisions in 2011 and 2012 at centre-of-mass energies of 7 and 8 TeV at the Large Hadron Collider (LHC) by the ATLAS¹ and CMS² detectors.

2 Production Asymmetries

The Tevatron forward-backward asymmetry measurements have initially shown some tension with the SM predictions^{3,4}. At the LHC, with a symmetric initial state, a charge asymmetry is measured, given by:

$$A_C = \frac{N(\Delta|y| > 0) - N(\Delta|y| < 0)}{N(\Delta|y| > 0) + N(\Delta|y| < 0)} \quad (1)$$

The charge asymmetry can be set up using the rapidity y of the top quarks ($\Delta|y| = |y_t| - |y_{\bar{t}}|$) or with the pseudo-rapidity η of the leptons in the dilepton channel (replacing $\Delta|y|$ with $\Delta|\eta| = |\eta_{l+}| - |\eta_{l-}|$). In the SM, the top-quark production asymmetries are due to NLO QCD interference effects. Measurements of A_{FB} at the Tevatron and A_C at the LHC have complementary sensitivity to new physics models^{5,6}. ATLAS presents two results in the lepton+jets channel at $\sqrt{s} = 8$ TeV. In one analysis⁷, a minimum $t\bar{t}$ invariant mass of 0.75 TeV is imposed, and the final state is selected by looking for a resolved leptonic top-quark decay and a hadronic decay which is reconstructed as a large R -jet with substructure where $R = \sqrt{(\Delta\eta)^2 + (\Delta\phi)^2}$. In the other presented analysis⁸, three signal regions are used based on the b-tag multiplicity. Full Bayesian unfolding is used to bring the distributions back to parton level. The inclusive charge asymmetry is measured as $A_C = [4.2 \pm 3.2 (\text{stat.} + \text{syst.})] \%$ ⁷ and

$A_C = [0.9 \pm 0.5 \text{ (stat. + syst.)}] \%$ ⁸. CMS also presents an analysis in the lepton+jets channel⁹ at $\sqrt{s} = 8 \text{ TeV}$. The charge asymmetry is measured with a template fit using symmetric and asymmetric templates of $\Upsilon_{t\bar{t}} = \tanh \Delta |y|_{t\bar{t}}$. The fit parameter α represents the relative contribution of the symmetric and asymmetric templates. This results in $A_C = [0.33 \pm 0.42 \text{ (stat. + syst.)}] \%$. CMS presents a result in the dilepton channel¹⁰, where the asymmetry is determined using the final-state leptons and reconstructed top quarks, leading to $A_C = [1.1 \pm 1.3 \text{ (stat. + syst.)}] \%$ based on the top quarks and $A_C^{\text{lep}} = [0.3 \pm 0.7 \text{ (stat. + syst.)}] \%$ based on the leptons. The results are observed to be consistent with the SM, as seen from the summary in Fig. 1a. In addition, all analyses provide differential measurements of the charge asymmetry in a variety of variables, e.g. invariant mass $m(t\bar{t})$, transverse momentum $p_T(t\bar{t})$ and velocity $\beta(t\bar{t})$ of the top-quark pair.

3 Spin Correlations

In top-quark pair production, the SM predicts the spins of the top- and antitop-quark to be correlated. The spin information of the top quark can be accessed using the decay products. ATLAS presents an analysis¹¹ making use of the following double differential cross section:

$$\frac{1}{N} \frac{d^2 N}{d \cos \theta_1 d \cos \theta_2} = \frac{1}{4} (1 + B_1 \cos \theta_1 + B_2 \cos \theta_2 - C_{\text{hel}} \cos \theta_1 \cos \theta_2) \quad (2)$$

where θ is the angle between the lepton direction in the top (anti-)quark parent rest frame and the top (anti-)quark parent in the $t\bar{t}$ rest frame. $B_{1,2}$ are proportional to the top-quark polarisation and are considered to be zero. Using this equation, the spin correlation strength A_{hel} can be directly extracted from $C_{\text{hel}} = -A_{\text{hel}} \alpha_1 \alpha_2$. ATLAS presents an analysis at $\sqrt{s} = 7 \text{ TeV}$ ¹¹ in the dilepton channel that results in $A_{\text{hel}} = 0.315 \pm 0.061 \text{ (stat.)} \pm 0.049 \text{ (syst.)}$. CMS presents an analysis at $\sqrt{s} = 8 \text{ TeV}$ ¹² in the dilepton channel where several asymmetry variables are used to perform a direct measurement of the spin correlation strength and the top-quark polarization. A measurement of the spin correlation strength can be interpreted in terms of several BSM models. As an example, the CMS measurement has been used to set limits on top-quark chromomagnetic couplings¹³ of $-0.053 < \text{Re}(\mu_t) < 0.026$ for the chromomagnetic dipole moment (CMDM) and $-0.068 < \text{Im}(d_t) < 0.067$ for the chromo-electric dipole moment (CEDM) both at the 95 % confidence level (CL). ATLAS presents an analysis at $\sqrt{s} = 8 \text{ TeV}$ ¹⁴ where the spin correlation measurement is interpreted in terms of a Minimal Super-Symmetric Model (MSSM) where stop squarks decay 100 % into a top quark and a neutralino with the stop squark mass very close to the top-quark mass. Stop squark masses between the top-quark mass and 191 GeV are excluded at the 95 % CL. CMS presents an analysis at $\sqrt{s} = 8 \text{ TeV}$ ¹⁵ in the lepton + jets channel where a matrix element method is used to set up a variable sensitive to spin correlation. Using matrix elements for $t\bar{t}$ production and decay using SM spin correlations and zero spin correlations, the likelihood ratio of these two hypotheses is used to perform a template fit and a hypothesis testing procedure. A SM fraction of $f^{SM} = 0.72 \pm 0.08 \text{ (stat.)} {}^{+0.15}_{-0.13} \text{ (syst.)}$ is measured.

4 Flavour-changing Neutral Currents

In the SM, FCNC are suppressed at tree-level due to the GIM mechanism. This leads to very small branching ratios of $t \rightarrow u/c + X$ with $X = g, \gamma, Z, H$ of $O(10^{-12} - 10^{-17})$. Several BSM models, such as MSSM, 2HDM, predict enhanced couplings for FCNC with branching ratios as high as 10^{-5} . With the discovery of the Higgs boson, FCNC can now also be studied in $t\bar{t}$ where one of the top quarks decays as $t \rightarrow u/c + H$. A clear overview of the predictions can be found in the reviews^{16,17}. CMS presents three analyses in this channel. One analysis¹⁸ makes use of the high branching fraction of $H \rightarrow b\bar{b}$ to look for $t\bar{t}$ production with decays of $t \rightarrow Hq \rightarrow b\bar{b}q$ in one leg and $t \rightarrow Wb \rightarrow \nu b$ in the other, obtaining an observed limit of

$B(t \rightarrow Hc) < 1.16\%$ and $B(t \rightarrow Hu) < 1.92\%$ at 95 % CL. Using the cleaner Higgs decay channel $H \rightarrow \gamma\gamma$ and looking for top-quark pairs with $t \rightarrow Hq \rightarrow \gamma\gamma q$ and $t \rightarrow Wb \rightarrow l\nu b$ or $q\bar{q}b$, observed limits are set of $B(t \rightarrow Hc) < 0.47\%$ and $B(t \rightarrow Hu) < 0.42\%$ at 95 % CL¹⁹. Finally, using $t\bar{t}$ events where $t \rightarrow Hq \rightarrow ZZq$ or WWq and $t \rightarrow Wq \rightarrow l\nu b$, CMS reports an observed limit of $B(t \rightarrow Hc) < 0.93\%$ at 95 % CL²⁰. ATLAS presents an analysis at $\sqrt{s} = 8$ TeV²¹ searching for FCNC in the channel $t \rightarrow Hq \rightarrow b\bar{b}q$ and $t \rightarrow Wb \rightarrow l\nu b$. Several signal categories are used based on jet and b-tag multiplicity. An observed limit of $B(t \rightarrow Hc) < 0.56\%$ and $B(t \rightarrow Hu) < 0.61\%$ is reported at the 95 % CL. In addition, a re-interpretation of previous $t\bar{t}H$ searches is performed in this analysis and combined limits are presented. Summaries of the observed limits on FCNC are shown in Fig. 1b-1d.

5 CP Violation

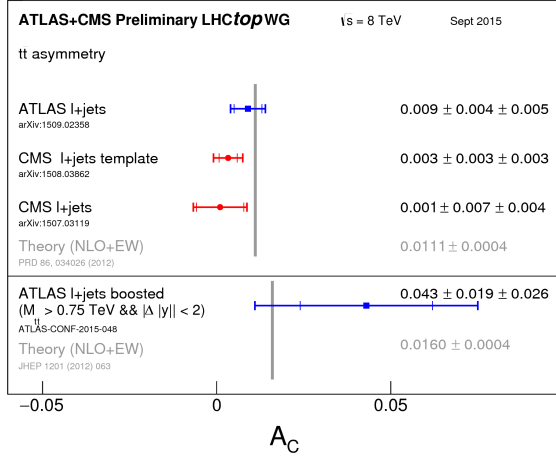
A first search for CP violation in the $t\bar{t}$ sector has been pursued by CMS in the l+jets channel by inspecting T-odd observables²². The observables are defined as $O_2 \propto (\vec{p}_b + \vec{p}_{\bar{b}}) \cdot (\vec{p}_l \times \vec{p}_{j1})$, $O_3 \propto Q_l \vec{p}_b \cdot (\vec{p}_l \times \vec{p}_{j1})$, $O_4 \propto Q_l (\vec{p}_b - \vec{p}_{\bar{b}}) \cdot (\vec{p}_l \times \vec{p}_{j1})$ and $O_7 \propto (\vec{p}_b - \vec{p}_{\bar{b}})_z (\vec{p}_b \times \vec{p}_{\bar{b}})_z$. The statistically limited results are found to be in agreement with no CP violation in $t\bar{t}$ production and decay, and the following values have been measured for A'_{CP} : $O_2 = +0.27 \pm 0.41$ (stat.) ± 0.01 (syst.), $O_3 = -0.71 \pm 0.41$ (stat.) ± 0.03 (syst.), $O_4 = -0.38 \pm 0.41$ (stat.) ± 0.03 (syst.), $O_7 = -0.06 \pm 0.41$ (stat.) ± 0.01 (syst.).

6 Conclusions

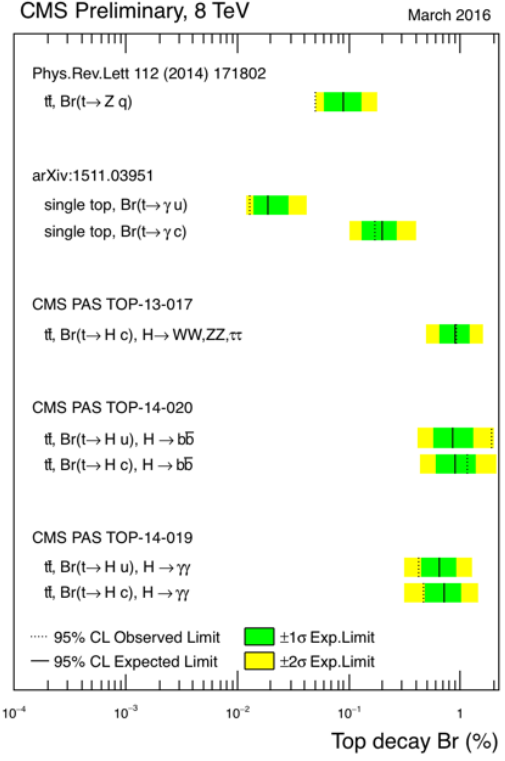
Top-quark properties measurements at the LHC provide precision tests of the SM. Limits have been set on FCNC and precision measurements of spin correlations and the charge asymmetry are consistent with the SM.

References

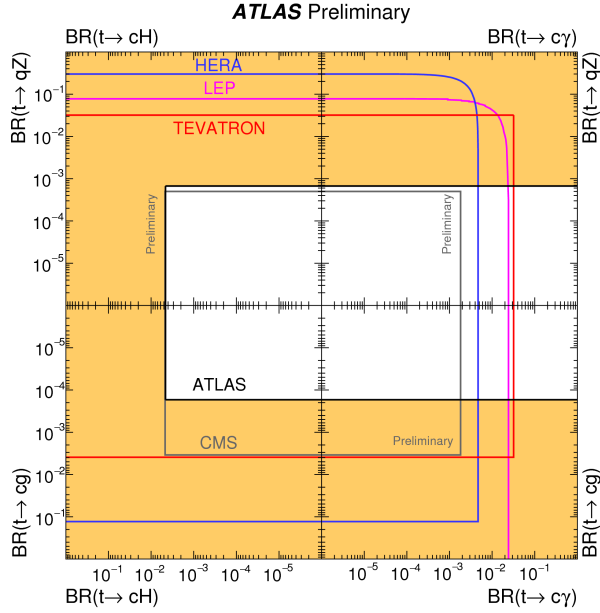
1. ATLAS Collaboration, JINST **3**, S08003 (2008).
2. CMS Collaboration, JINST **3**, S08004 (2008).
3. D0 Collaboration, *Phys. Rev. Lett.* **100**, 142002 (2008).
4. CDF Collaboration, *Phys. Rev. Lett.* **101**, 202001 (2008).
5. Aguilar-Saavedra J. A. and Pérez-Victoria M., *Phys. Rev. D* **84**, 115013 (2011).
6. Aguilar-Saavedra J. A. and Pérez-Victoria M., *JHEP* **09**, 097 (2011).
7. ATLAS Collaboration, *Phys. Lett. B* **756**, 52 (2016).
8. ATLAS Collaboration, *Eur. Phys. J. C* **76**, 87 (2016).
9. CMS Collaboration, *Phys. Rev. D* **93**, 034014 (2016).
10. CMS Collaboration, arXiv:1603.06221 (2016), submitted to PLB
11. ATLAS Collaboration, *Phys. Rev. D* **93**, 012002 (2016).
12. CMS Collaboration, *Phys. Rev. D* **93**, 052007 (2016).
13. W. Bernreuther and Z.-G. Si, *Phys. Lett. B* **725**, 115-122 (2013).
14. ATLAS Collaboration, *Phys. Rev. Lett.* **114**, 142001 (2015).
15. CMS Collaboration, arXiv:1511.06170 (2015), submitted to PLB
16. Aguilar-Saavedra J., *Acta Phys. Polon. B* **35**, 2695 (2004).
17. Larios F., Martinez R. and Pérez M., *Int. J. Mod. Phys. A* **21**, 3473-3494 (2006).
18. CMS Collaboration, CMS-PAS-TOP-14-020.
19. CMS Collaboration, CMS-PAS-TOP-14-019.
20. CMS Collaboration, CMS-PAS-TOP-13-017.
21. ATLAS Collaboration, *JHEP* **12**, 061 (2015).
22. CMS Collaboration, CMS-PAS-TOP-16-001.



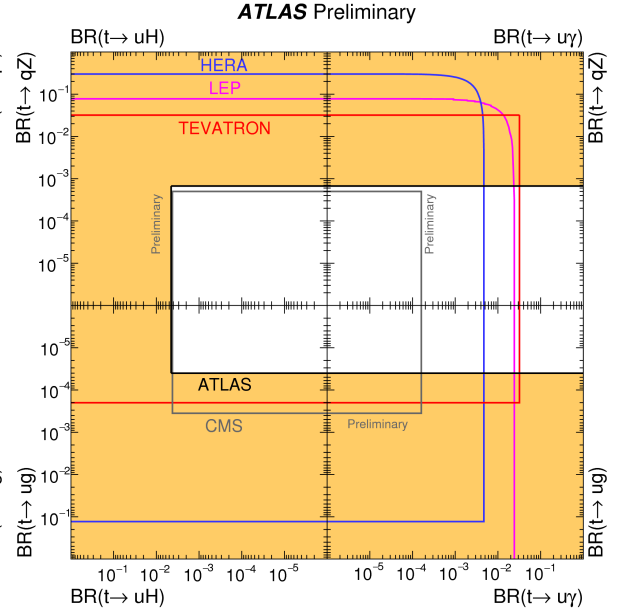
(a) Summary of top charge asymmetry



(b) Summary of FCNC limits in CMS



(c) Summary of FCNC limits in ATLAS $t \rightarrow cX$



(d) Summary of FCNC limits in ATLAS $t \rightarrow uX$

Figure 1: Summary of top charge asymmetry measurements at $\sqrt{s} = 8$ TeV at ATLAS and CMS in Fig. 1a. Summary of the limits on FCNC for CMS in Fig. 1b and ATLAS in Fig. 1c-1d. In the ATLAS summary plots, the orange exclusion region narrows down to smaller branching ratios at the centre of the plot, while in the CMS summary plot the excluded region is on the right of the observed branching ratio limits.